Available online at www.sciencedirect.com
SCIENCE DIRECT®
Journal of Magnetic Resonance 168 (2004) 147–152
JMR Journal of Magnetic Resonance
www.elsevier.com/locate/jmr

Cross-polarization schemes for peptide samples oriented in hydrated phospholipid bilayers

Hyeongnam Kim,[a,b] Timothy A. Cross,[a,b,c] and Riqiang Fu[a,*]

[a] *Center for Interdisciplinary Magnetic Resonance, Florida State University, National High Magnetic Field Laboratory, 1800 E. Paul Dirac Drive, Tallahassee, FL 32310, USA*
[b] *Department of Chemistry and Biochemistry, Florida State University, Tallahassee, FL 32306, USA*
[c] *Institute of Molecular Biophysics, Florida State University, Tallahassee, FL 32306, USA*

Received 5 December 2003; revised 6 February 2004

Abstract

Continuous-wave, ramped amplitude, and frequency modulated cross-polarization schemes (abbreviated as CWCP, RACP, and FMCP, respectively) are evaluated for static samples in anisotropic phases, such as peptides oriented in lipid environments. It is shown experimentally that both RACP and FMCP give rise to 20% higher polarized signal intensity in comparison to CWCP. The CP matching bandwidths for CWCP and RACP are about the same. Because of its adiabaticity, FMCP has a much broader CP matching bandwidth than CWCP and RACP. In addition, the ^{15}N RF amplitude used at the center of the FMCP matching profile is much lower than that of the CWCP and RACP matching profiles. A sample of [^{15}N]Leu$_4$ labeled gramicidin A oriented in lipid bilayers was used to demonstrate these experiments.

Keywords: Ramped amplitude CP; Frequency modulated CP; Solid-state NMR; Peptide; Aligned lipid bilayers

1. Introduction

Cross-polarization (CP) [1] has been widely used to enhance the polarization of dilute nuclei, S with low gyromagnetic ratios from abundant nuclei, I with higher gyromagnetic ratios. Efficient CP transfer is generally achieved by spin-locking both the I and S spins with radiofrequency (RF) amplitudes that fulfill the Hartmann–Hahn match condition $\omega_{1I} = \omega_{1S}$ [2], where ω_{1I} and ω_{1S} refer to the amplitudes of the RF fields applied to the I and S spins, respectively. The matching bandwidth is dictated by the I–S heteronuclear interactions (including dipolar and scalar interactions), as well as the ^{1}H homonuclear dipolar interactions [3]. In solids, the Hartmann–Hahn match condition is relatively easy to fulfill because of the presence of strong dipolar couplings. In contrast, although CP can also be very useful in isotropic liquids to transfer coherence between scalar-coupled nuclei [4,5], other techniques such as the Overhauser effect [6,7] and INEPT [8,9] are primary means for the heteronuclear polarization transfer in liquids. This is because weak scalar couplings in liquids make the Hartmann–Hahn match condition very difficult to achieve, thus greatly decreasing the CP efficiency. Here, cross-polarization suitable for samples in static anisotropic phases, such as liquid crystals and membrane proteins oriented in hydrated lipid environments, is discussed.

It has been well known in CP magic angle spinning (MAS) NMR that as long as the spinning speed is much smaller than the homogeneous linewidth of the I spins, spin diffusion among the I spins is as efficient as in static solids, so that the Hartmann–Hahn match condition can be violated without dramatic consequences. In other words, the Hartmann–Hahn matching bandwidth is very broad. However, when the spinning speed is comparable to, or larger than, the linewidth of the I spins, the Hartmann–Hahn match condition is broken into a series of sidebands separated by the spinning speed [10]. The width of these sidebands is much narrower than the matching bandwidth for a static sample. Under these

* Corresponding author. Fax: 1-850-6441366.
E-mail address: rfu@magnet.fsu.edu (R. Fu).

1090-7807/$ - see front matter © 2004 Elsevier Inc. All rights reserved.
doi:10.1016/j.jmr.2004.02.010

conditions, the matching condition tends to be very sensitive to experimental imperfections such as RF inhomogeneities and amplifier instabilities during long duration experiments thus significantly reducing the CP efficiency [11].

Many spectroscopic approaches have been proposed in the past decades to enhance the CP efficiency in both solid-state static and MAS NMR by broadening the Hartmann–Hahn match condition [12–20]. For instance, amplitude modulation [12,13] and frequency modulation [14–16] have been used to broaden the Hartmann–Hahn match condition under fast MAS. In static samples, MOIST [17,18], adiabatic schemes such as adiabatic passage [19] and variable-amplitude CP [20] have been used to improve the CP efficiency. However, some spin properties for samples in anisotropic phases such as liquid crystals and membrane proteins oriented in hydrated lipid environments are quite different from those in rigid solids [21]. Thus, many CP methods developed for static or MAS solid-state NMR may not necessarily be optimal for anisotropic phases. For example, a sample of gramicidin A oriented in hydrated lipid environments experiences a significant degree of dynamics so that the CP match condition tends to be very critical even without sample spinning. Moreover, the ^{1}H spin–lattice relaxation time in the rotating frame ($T_{1\rho}$) is typically on the order of a few milliseconds [22]. Since the adiabatic CP schemes used in static solids usually require a relatively long CP contact time to fulfill the adiabatic condition [19], they can hardly be applied to these anisotropic phases. Furthermore, the presence of high hydration in the anisotropic phases absorbs considerable RF energy so that sample heating becomes very significant especially under strong RF irradiation. Thus it is highly desirable to use low RF amplitude during spectroscopic measurements of such samples. It has been demonstrated that CP can become very efficient [23] in isotropic liquids when the RF amplitudes are comparable to the heteronuclear scalar coupling constants, which are on the order of a hundred Hertz. However, such low RF amplitudes are not appropriate for spin-locking in the anisotropic phases exhibiting much stronger interactions. In addition, due to the nature of aligned membrane protein samples, a large rectangular sample coil is typically used to acquire weak NMR signals. For such coils RF inhomogeneities across the sample region may be very significant and the Hartmann–Hahn match condition may become impossible to achieve over the entire sample region with standard cross-polarization methods.

In this work, we apply three CP schemes to aligned membrane samples in a liquid crystalline phase, continuous-wave CP (CWCP), ramped-amplitude CP (RACP) [24], and frequency modulated CP (FMCP) [14,15]. Their CP efficiencies will be evaluated and discussed using a ^{15}N-labeled gramicidin A sample oriented in hydrated lipid bilayers. Gramicidin A (gA) is a polypeptide of 15 amino acid residues, whose high-resolution structure in lipid bilayers has been uniquely defined using 120 orientational restraints from solid-state NMR [25,26].

2. Materials and experiments

An oriented [^{15}N]Leu$_4$ labeled gramicidin A (gA) sample was prepared by codissolving 10 mg gA and 30 mg dimyristoylphosphatidylcholine (DMPC) in 1.5 ml 95/5 (v/v) benzene/ethanol solution. Thirty microliters of the solution was spread on each of 50 glass slides ($5.7 \times 12.0 \times 0.07\,\text{mm}^3$), following which the solvents were partially evaporated in air at room temperature. Drying was completed overnight in a vacuum. These glass slides were then stacked in a square glass tube (with inner dimension of $6.0 \times 6.0 \times 15.0\,\text{mm}^3$). The tube was sealed after adding 50% HPLC-grade H_2O (by total sample dry weight) and incubated at 43 °C until the sample became transparent and uniformly hydrated [27]. The sample was placed in the magnetic field such that the normal to the lipid bilayers was parallel to B_0.

All NMR measurements were carried out at 30 °C on a 400 MHz NMR spectrometer with a Bruker DRX console, equipped with a homebuilt wideline ^{1}H–^{15}N double resonance NMR probe using a large rectangular sample coil ($8 \times 8 \times 12\,\text{mm}^3$). The coil was directly wound on the sample tube using copper foil in order to enhance the RF performance of the probe. The Larmor frequencies of ^{1}H and ^{15}N are 400.1 and 40.5 MHz, respectively. Brey et al. [28] evaluated the RF inhomogeneities by measuring the signal intensities in a single-pulse experiment as a function of flip angle, up to 810°. They reported that the intensity ratios, $A_{810°}/A_{90°}$ were 0.78 for ^{15}N and 0.40 for ^{1}H with a large sample coil ($8 \times 8 \times 12\,\text{mm}^3$). The ^{15}N RF spin-lock amplitudes in the experiments were determined via measurement of the 180° pulse length at different RF input power levels, while matching the ^{1}H RF spin-lock amplitude calibrated to be 38.5 kHz by measurement of the ^{1}H 180° pulse length via indirect observation of the ^{15}N signals through CP.

^{15}N signals were observed at 145 ppm with respect to 0 ppm for a saturated solution of $^{15}NH_4NO_3$ [25]. For each experiment, 4096 scans were accumulated with a recycle delay of 5 s during continuous-wave proton decoupling with an RF amplitude of 38.5 kHz. The contact time used was 600 μs in all measurements. The ^{15}N RF amplitude was varied in order to obtain the matching bandwidths for the three CP schemes. For CWCP, both the ^{15}N RF amplitude and its frequency are kept constant during the individual experiments. For the RACP scheme, the ^{15}N RF amplitude is ramped from 80 to 100% of the maximum RF amplitude, but its carrier

frequency is kept constant. For FMCP, the ^{15}N carrier frequency is modulated by a single cycle of a sine wave over the CP contact time, while its RF amplitude is kept constant. The average of the frequency modulation is positioned in the center of the ^{15}N NMR spectrum. In our experiments, the depth of the frequency modulation used was 50 kHz and 2048 steps were used to digitize this modulation over the CP contact time. The waveform for the frequency modulation was generated using a C program and transferred to the waveform generator.

3. Results and discussion

Fig. 1 shows CP optimized ^{15}N spectra of ^{15}N-Leu$_4$ gramicidin A (gA) oriented in DMPC (1:8 molar ratio) bilayers using three CP schemes. ^{15}N signal intensities obtained by RACP and FMCP are about 25 and 20% larger, respectively, than that by CWCP. The ^{15}N spin-lock RF amplitude used in the CWCP experiment is about the same as the average ^{15}N RF amplitude in the RACP measurement, while the optimized ^{15}N RF amplitude in the FMCP spectrum appears to be more than 2 kHz lower than in CWCP and RACP. It is worth noting that in oriented samples the transfer of magnetization from the I to S spins oscillates with respect to the contact time [22,29]. Therefore, a CP contact time needs to be carefully chosen for maximum polarization transfer [30]. Since the transient dipolar oscillation depends on the heteronuclear dipolar coupling between the I and S spins, it would be preferable to choose a relatively long contact time to avoid the oscillatory period in order to maximize signals for various sites. With the sample used here, the transient dipolar oscillation was damped almost completely at a contact time of 600 μs by the proton–proton spin diffusion. Therefore, such a contact time was chosen for our measurements. A longer contact time further decreases the signal intensity because the gA sample exhibits a relatively short ^{1}H spin–lattice relaxation time in the rotating frame [22,31].

Fig. 2 shows the plot of ^{15}N intensities as a function of RF amplitude in the three different schemes. The CP matching bandwidth for CWCP is about 12 kHz, measured at 70% of the maximum CWCP signal height, much narrower than what is normally observed in rigid solid samples [3]. This implies the presence of a significant degree of dynamics in the hydrated gA sample that reduces the dipolar interactions. It is surprising from Fig. 2 that the CP matching bandwidth for RACP is increased only slightly to 14 kHz compared to that for CWCP when the average RF amplitude for RACP, which corresponds to 90% of the maximum RF amplitude, is used for the abscissa. Furthermore, the center of the match profile appears at the optimal Hartmann–Hahn match condition (i.e., $\omega_{1N}/2\pi = \omega_{1H}/2\pi = 38.5$ kHz), even though RACP clearly polarizes more of the

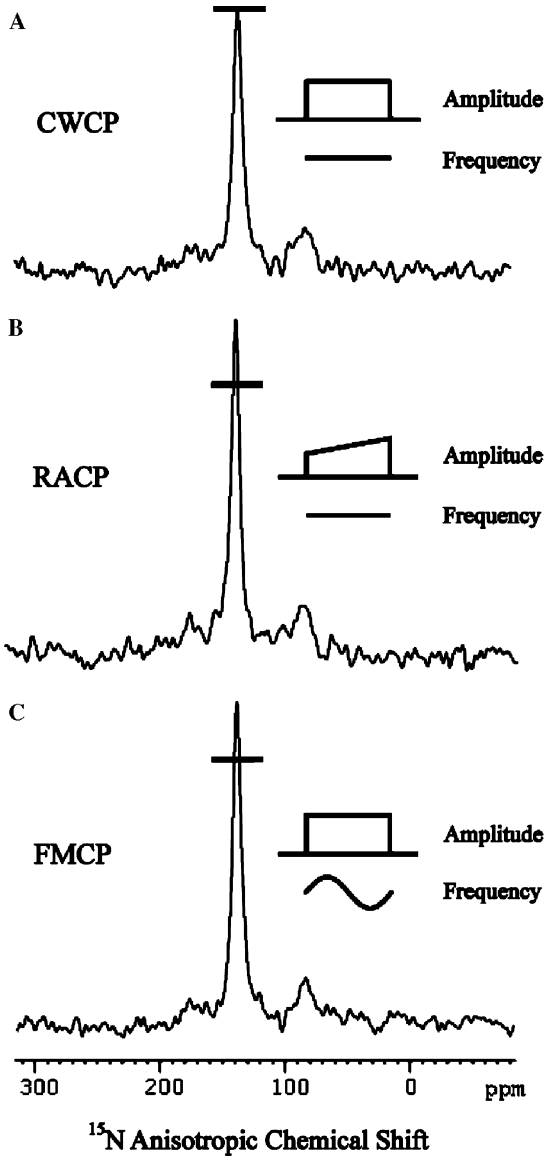

Fig. 1. Optimized ^{15}N NMR spectra of ^{15}N-Leu$_4$ gramicidin A oriented (1:8 molar ratio) in DMPC using different CP schemes: (A) CWCP, (B) RACP, and (C) FMCP. The bar () on the spectra indicates the peak height of the CWCP spectrum. In the CWCP experiment, the optimal ^{15}N signal was obtained with the ^{15}N RF spin-lock amplitude of 38.4 kHz. In the RACP experiment, the optimal ^{15}N signal intensity was achieved when the ^{15}N RF amplitude was ramped between 34.5 and 43.1 kHz, corresponding to an average amplitude of 38.8 kHz. While in FMCP, an ^{15}N RF amplitude of 36.3 kHz gives rise to maximum polarization for the ^{15}N signal.

sample than CWCP. This is different from examples of RACP in fast MAS cases of solid samples where RACP exhibits a much broader matching bandwidth compared to CWCP [24]. For FMCP, the CP matching profile is dramatically broader than that in CWCP and RACP. The range of ^{15}N RF amplitude resulting in 70% of the CWCP signal intensity is broadened by a factor of 2.8 compared to CWCP. As a result, the CP efficiency tends to be less sensitive to the RF inhomogeneities as well as

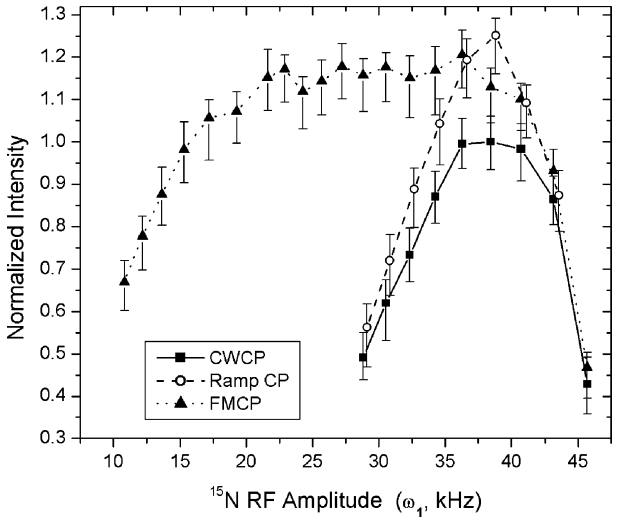

Fig. 2. ^{15}N intensities as a function of RF amplitude with the three different schemes: CWCP (■), RACP (○), and FMCP (▲). All intensities were normalized to the maximum signal obtained by CWCP at the ^{15}N RF amplitude of 38.4 kHz. Average RF amplitudes are used for RACP in the plot. The error bars were calculated based on the noise levels in the spectra.

the resonance offsets for both channels. In the center of the matching profile for FMCP, the ^{15}N RF amplitude is 28.5 kHz, much lower than that for CWCP and RACP. This generates a significant advantage for cross-polarization, because it is technically difficult when using an NMR probe with a large sample coil to generate high ^{15}N RF amplitudes due to its low gyromagnetic ratio. For CWCP and RACP, the ^{15}N RF amplitude generated by the large sample coil may be a limiting factor for setting the ^{1}H RF amplitude during CP. Therefore, for FMCP a much higher ^{1}H RF amplitude can be used for CP even if a limited ^{15}N RF amplitude is achieved by the probe. The higher ^{1}H RF amplitude will lead to a longer ^{1}H spin–lattice relaxation time in the tilted rotating frame that gives rise to less decay of the ^{1}H magnetization in the tilted rotating frame so as to increase the polarized signal intensities [32].

Since we used a large rectangular sample coil ($8 \times 8 \times 12\,\mathrm{mm}^3$), the presence of RF inhomogeneities across the sample region especially for ^{1}H is anticipated. Therefore, it would be difficult to fulfill the exact Hartmann–Hahn match condition over the entire sample volume with CWCP. In other words, the CWCP efficiency will vary across the sample. MOIST [17,18] improves the CP efficiency under inhomogeneous RF fields by inverting the two spin-lock fields simultaneously during CP. Our experiments showed that the signal intensities obtained by MOIST were about 90% of that obtained by CWCP, although the former broadened the CP matching bandwidth by a factor of two in comparison with the latter (spectra not shown). Therefore, FMCP appears to be the best method for achieving an excellent and stable Hartmann–Hahn match condition for these hydrated bilayer samples observed in a liquid crystalline state. This is particularly important for low sensitivity samples, since the hydration level greatly affects the sample properties thus making cross polarization parameters difficult and very time-consuming to set up.

To understand the FMCP matching profile, the adiabaticity and the average effective ^{15}N spin-lock amplitude under frequency modulation has been examined. The degree to which the adiabatic condition is satisfied can be quantified by introducing the adiabaticity factor Q [33–37]

$$Q = \frac{|\omega_{\mathrm{eff}}(t)|}{|\mathrm{d}\theta/\mathrm{d}t|}, \tag{1}$$

where $\omega_{\mathrm{eff}}(t)$ is the ^{15}N transient RF amplitude and $\mathrm{d}\theta/\mathrm{d}t$ defines the change of the transient RF field. If we consider the sine wave modulation as used in our experiments, the minimum Q value over the modulation can be derived as [14]

$$Q_{\min} = \frac{\omega_1^2 \tau_{\mathrm{CP}}}{2\pi\omega_{\Delta}}, \tag{2}$$

where ω_1 is the ^{15}N RF amplitude, ω_{Δ} is the depth of the frequency modulation, and τ_{CP} is the CP contact time. When $Q \gg 1$, the adiabatic condition is fulfilled.

The transient ^{15}N RF amplitude for FMCP is defined by

$$\omega_{\mathrm{eff}}(t) = \sqrt{\omega_1^2 + [\omega_{\Delta}\sin(2\pi t/\tau_{\mathrm{CP}})]^2}. \tag{3}$$

Thus the average value of the effective field can be calculated by

$$\bar{\omega}_{\mathrm{eff}} = \frac{1}{\tau_{\mathrm{CP}}}\int_0^{\tau_{\mathrm{CP}}} \omega_{\mathrm{eff}}\,\mathrm{d}t. \tag{4}$$

It has been known that the effective field can be greatly increased by using frequency offset and an experimental strategy utilizing the frequency offset has been used during CP to dramatically reduce the RF power used in CP [38,39]. Thus, when the amplitude modulation (e.g., the ramped amplitude) is combined with a relatively large frequency offset, it is possible that the CP efficiency might become less sensitive to the applied RF amplitude due to the contribution of the constant frequency offset to the effective field, provided that the adiabaticity is somehow fulfilled. In this case, an ^{15}N RF pulse is required at the end of the CP contact to flip the polarized magnetization onto the x–y plane for detection [38,39]. For the frequency modulation used here, the effective RF spin-lock field is always larger than the applied RF amplitude, as indicated in Eq. (3). Fig. 3 shows the Q value and the average field for FMCP at different RF amplitudes. We used $\omega_{\Delta}/2\pi = 50$ kHz, $\tau_{\mathrm{CP}} = 600\,\mu$s and $\omega_1/2\pi$ ranging from 10 to 45 kHz in the simulations. From Eq. (2), when $\omega_1/2\pi = 45$ kHz, the adiabatic condition is fulfilled with $Q = 24.3 \gg 1$.

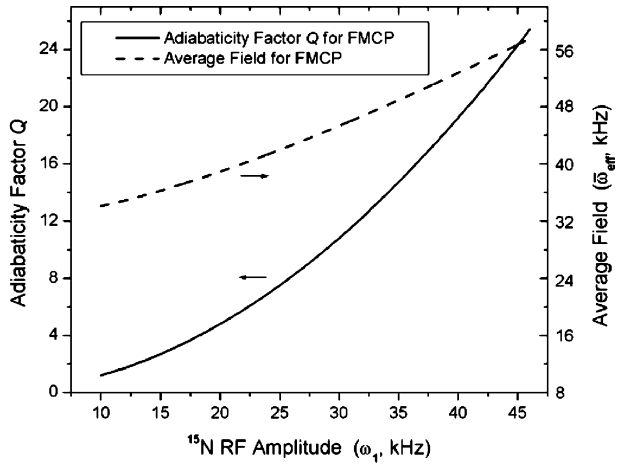

Fig. 3. Q value and average field for FMCP: solid line indicates Q value and dashed line for average field. Q is the adiabaticity factor obtained from Eq. (2) and the average field is obtained from Eq. (4).

However, when $\omega_1/2\pi = 10$ kHz, the adiabatic condition is not well met, $Q = 1.2$. Consequently the polarized ^{15}N signal intensity at very low ^{15}N RF amplitude (e.g., 13 kHz) is less than that at high ^{15}N RF amplitude (e.g., 40 kHz), resulting in an asymmetric CP matching profile for FMCP, as shown in Fig. 2. Fig. 3 shows that the change of the average field for FMCP is less sensitive to the ^{15}N RF amplitude. When the ^{15}N RF amplitude is 44 kHz, the average field is 56 kHz. An ^{15}N RF amplitude of 13 kHz corresponds to an average field of 35 kHz. Therefore, FMCP has a matching profile ranging from 13 to 44 kHz (a 31 kHz range), while the average field is in the range 35–56 kHz (a 21 kHz range). Even the matching range of the average field is nearly twice as broad as that for CWCP and RACP. The average field for FMCP depends on the modulation parameters and on the ^{15}N RF amplitude. With a larger ω_Δ, the average field becomes less dependent on the ^{15}N RF amplitude. For instance, when $\omega_\Delta/2\pi = 40$ kHz and $\omega_1/2\pi$ is from 13 to 44 kHz (a 31 kHz range), the calculated average field based on Eq. (4) is from 29 to 52 kHz (a 23 kHz range). While at $\omega_\Delta/2\pi = 60$ kHz with the same range of $\omega_1/2\pi$, the average field is from 41 to 60 kHz (a 19 kHz range). However, the adiabatic condition becomes relatively difficult to fulfill at a large ω_Δ, as indicated in Eq. (2), especially when ω_1 is low.

4. Conclusions

We have evaluated the cross-polarization of CWCP, RACP, and FMCP as applied to peptide samples oriented in hydrated phospholipid bilayers in terms of cross-polarization efficiency and cross-polarization matching bandwidth. It is shown experimentally that FMCP and RACP give rise to 20 and 25%, respectively, more ^{15}N signal than CWCP. Both CWCP and RACP show the same narrow CP matching bandwidth as a function of ^{15}N RF amplitude while FMCP exhibits a much broader matching bandwidth whether measured as a function of RF amplitude or as a function of average field. The use of FMCP allows us to optimize the CP condition easily in low sensitivity samples and to save considerable time in the spectrometer set up. Moreover, the ^{15}N RF amplitude used in FMCP can be significantly lower than in CWCP and RACP, thus reducing sample heating due to RF irradiation. Alternatively, FMCP can allow for much higher ^{1}H irradiation to achieve better $T_{1\rho}$ while allowing nearly optimal cross-polarization.

Acknowledgments

This work was supported in part by the National Science Foundation MCB 02-35774 and the work was performed at the National High Magnetic Field Laboratory supported by the National Science Foundation Cooperative Agreement DMR-0084173 and the State of Florida. We gratefully acknowledge helpful comments by the referees.

References

[1] A. Pines, M.G. Gibby, J.S. Waugh, Proton-enhanced NMR of dilute spins in solids, J. Chem. Phys. 59 (1973) 569–590.
[2] S.R. Hartmann, E.L. Hahn, Nuclear double resonance in the rotating frame, Phys. Rev. 128 (1962) 2042–2053.
[3] E.O. Stejskal, J. Schaefer, J.S. Waugh, Magic-angle spinning and polarization transfer in proton-enhanced NMR, J. Magn. Reson. 28 (1977) 105–112.
[4] A.A. Maudsley, L. Müller, R.R. Ernst, Cross-correlation of spin-decoupled NMR spectra by heteronuclear two-dimensional spectroscopy, J. Magn. Reson. 28 (1977) 463–469.
[5] L. Müller, R.R. Ernst, Coherence transfer in the rotating frame. Application to heteronuclear cross-correlation spectroscopy, Mol. Phys. 38 (1979) 963–992.
[6] A.W. Overhauser, Polarization of nuclei in metals, Phys. Rev. 92 (1953) 411–415.
[7] I. Solomon, Relaxation processes in a system of two spins, Phys. Rev. 99 (1955) 559–565.
[8] R.D. Bertrand, W.B. Moniz, A.N. Garroway, G.C. Chingas, ^{13}C–^{1}H cross-polarization in liquids, J. Am. Chem. Soc. 100 (1978) 5227–5229.
[9] M. Ernst, C. Griesinger, R.R. Ernst, W. Bermel, Optimized heteronuclear cross polarization in liquids, Mol. Phys. 94 (1991) 219–252.
[10] M. Sardashti, G.E. Maciel, Effects of sample spinning on cross polarization, J. Magn. Reson. 72 (1987) 467.
[11] K. Nishimura, R. Fu, T.A. Cross, The effect of RF inhomogeneity on heteronuclear dipolar recoupling in solid state NMR: practical performance of SFAM and REDOR, J. Magn. Reson. 152 (2001) 227–233.
[12] S. Hediger, B.H. Meier, R.R. Ernst, Cross polarization under fast magic angle sample spinning using amplitude-modulated spin-lock sequences, Chem. Phys. Lett. 213 (1993) 627–635.

[13] O.B. Peersen, X. Wu, I. Kustanovich, S.O. Smith, Variable-amplitude cross polarization MAS NMR, J. Magn. Reson. A 104 (1993) 334–339.
[14] R. Fu, P. Pelupessy, G. Bodenhausen, Frequency-modulated cross-polarization for fast magic angle spinning NMR at high field: relaxing the Hartmann–Hahn condition, Chem. Phys. Lett. 264 (1997) 63–69.
[15] A.C. Kolbert, A. Bielecki, Broadband Hartmann–Hahn matching in magic-angle spinning NMR via an adiabatic frequency sweep, J. Magn. Reson. A 116 (1995) 29–35.
[16] S. Hediger, B.H. Meier, R.R. Ernst, Adiabatic passage Hertmann-Hahn cross polarization in NMR under magic angle spinning, Chem. Phys. Lett. 240 (1995) 449–456.
[17] M.H. Levitt, D. Suter, R.R. Ernst, Spin dynamics and thermodynamics in solid-state NMR cross polarization, J. Chem. Phys. 84 (1986) 4243–4255.
[18] S. Zhang, B.H. Meier, S. Appelt, M. Mehring, R.R. Ernst, Transient oscillations in phase-switched cross-polarization experiments, J. Magn. Reson. A 101 (1993) 60–66.
[19] S. Hediger, B.H. Meier, N.D. Kurur, G. Bodenhausen, R.R. Ernst, NMR cross polarization by adiabatic passage through the Hartmann Hahn condition (APHH), Chem. Phys. Lett. 223 (1994) 283–288.
[20] S. Zhang, Quasi-adiabatic polarization transfer in solid-state NMR, J. Magn. Reson. A 110 (1994) 73–76.
[21] D.E. Warschawski, P.F. Devaux, Polarization transfer in lipid membranes, J. Magn. Reson. 145 (2000) 367–372.
[22] F. Tian, T.A. Cross, Dipolar oscillations in cross-polarized peptide samples in oriented lipid bilayers, J. Magn. Reson. 125 (1997) 220–223.
[23] E. Chiarparin, P. Pelupessy, G. Bodenhausen, Selective cross-polarization in solution state NMR, Mol. Phys. 95 (1998) 759–767.
[24] G. Metz, X. Wu, S.O. Smith, Ramped-amplitude cross polarization in magic-angle-spinning NMR, J. Magn. Reson. A 110 (1994) 219–227.
[25] R. Ketchem, W. Hu, T.A. Cross, High-resolution conformation of gramicidin A in a lipid bilayer by solid state NMR, Science 261 (1993) 1457–1460.
[26] R.R. Ketchem, B. Roux, T.A. Cross, High-resolution polypeptide structure in a lameller phase lipid environment from solid state NMR derived orientational constraints, Structure 5 (1997) 1655–1669.
[27] R. Fu, C. Tian, H. Kim, S.A. Smith, T.A. Cross, The effect of Hartmann–Hahn mismatching on polarization inversion spin exchange at the magic angle, J. Magn. Reson. 159 (2002) 167–174.
[28] W.W. Brey, P.L. Gor'kov, C. Tian, R. Fu, T.A. Cross, Improvements in NMR probes for membrane protein studies, 43rd ENC, 2002.
[29] R. Pratima, K.V. Ramanathan, The application to liquid crystals of transient oscillations in cross polarization experiments, J. Magn. Reson. A 118 (1996) 7–10.
[30] S.C. Shekar, A. Ramamoorthy, The unitary evolution operator for cross-polarization schemes in NMR, Chem. Phys. Lett. 342 (2001) 127–134.
[31] R. Fu, C. Tian, T.A. Cross, NMR spin locking of proton magnetization under frequency switched Lee–Goldburg (FSLG) pulse sequence, J. Magn. Reson. 154 (2002) 130–135.
[32] R. Fu, J. Hu, T.A. Cross, Towards quantitative measurements in solid state CPMAS NMR: a Lee–Goldburg frequency modulated cross polarization scheme, J. Magn. Reson. 168 (2004) 8–17.
[33] A. Tannus, M. Garwood, Improved performance of frequency-swept pulses using offset-independent adiabaticity, J. Magn. Reson. A 120 (1996) 133–137.
[34] A. Tannus, M. Garwood, Adiabatic pulses, NMR Biomed. 10 (1997) 423–434.
[35] M. Garwood, L. DelaBarre, The return of the frequency sweep: designing adiabatic pulses for contemporary NMR, J. Magn. Reson. 153 (2001) 155–177.
[36] T.-L. Hwang, P.C.M. van Zijl, M. Garwood, Fast broadband inversion by adiabatic pulses, J. Magn. Reson. 133 (1998) 200–203.
[37] E. Kupce, R. Freeman, Optimized adiabatic pulses for wideband spin inversion, J. Magn. Reson. A 118 (1996) 299–303.
[38] S.C. Shekar, D.K. Lee, A. Ramamoorthy, An experimental strategy to dramatically reduce the RF power used in cross polarization solid-state NMR spectroscopy, J. Am. Chem. Soc. 123 (2001) 7467–7468.
[39] S.C. Shekar, D.K. Lee, A. Ramamoorthy, Chemical shift anisotropy and offset effects in cross polarization solid-state NMR spectroscopy, J. Magn. Reson. 157 (2002) 223–234.